USE OF GRAVITY, MICROEARTHQUAKE, AND TRACER INJECTION TEST DATA IN CALIBRATING THE TIWI NUMERICAL RESERVOIR MODEL

Cinco, Fra-Olalem R.[1], Marcuap, Harly L.[1], and Menzies, Anthony J.[1]

[1]Philippine Geothermal Production Company, Inc. 14th floor, 6750 Building Ayala Avenue, Makati City, Philippines 1226

fra.cinco@pgpc.com.ph

Keywords: *Tiwi, reservoir model, numerical modeling, geothermal model, precision gravity, microearthquake, tracer injection, conceptual model*

ABSTRACT

The Tiwi Geothermal Field, operated by Philippine Geothermal Production Company, Inc. (PGPC) in Albay, Philippines, has been in production since 1979 and the numerical model of the reservoir has been adequately matched to the collected production and injection history, including changes in subsurface pressure and temperature data as well as discharge enthalpies. The numerical reservoir model is based on the TOUGH2 simulation code and uses a double porosity formulation, with various levels of matrix block sub-division (MINC'ing) in the reservoir section.

In addition to matching the usual production and downhole survey data, matching of the changes in gravity, which have been precisely measured across the field for the past 40 years, is also routinely conducted. It has proven to be useful in providing additional insights into the reservoir processes taking place, particularly related to phase change, movement of the steam-water interface in the reservoir and the degree of mass influx, either from external aquifers or internally from matrix to the producing fractures. The matrix to fracture interactions are controlled in the model by parameters such as the fracture spacing, degree of MINC'ing of the matrix blocks and the permeabilities of the matrix and fractures.

Another geoscientific data set that is used to constrain the model is microearthquakes (MEQs). These are very low intensity earthquakes that can only be detected by precision instruments. Some of the MEQs are induced by injection, and to a lesser extent by production. We believe the distribution of these events indicates where rock-fluid heat exchange is occurring, and the existence and/or stimulation of the fracture network. Production and geochemical data during the past 20 years indicates a strong connection between edgefield injection wells in the southeast Naglagbong sector (where about 70% of the total brine is injected) and production wells in the South Kapipihan sector. Both the data and the model indicate that the injection in Naglagbong provides long-term pressure support to South Kapipihan with no negative thermal effects. The great depth and lateral extent of the MEQ activity readily explains this favorable behavior, as the result of a large volume of hot, fractured rock that allows for ample heat exchange before the injected brine reaches the production wells. The model has been adjusted to account for this volume, with consequences for reservoir volume and reserves.

More recently, a binary project has been proposed which will lower injection temperatures. Although the match in the model to pressure and temperature changes in the area has been generally good, it was found by tagging the injection water that the velocity of fluid movement in the model was not consistent with available tracer test results. To improve the calibration of the model and make it more consistent with tracer arrival times and concentration trends, it was necessary to add a streak of high permeability blocks that corresponds to a mapped fault (Cale Fault) to act as a conduit of fluids between the injection and production wells used in the tracer test.

The inclusion of both production and geoscientific data in calibrating the numerical model of Tiwi has resulted in improvements in the history matching and the simulation of reservoir processes, increasing confidence in the model's output and the use of the model to provide input to resource development decisions.

1. INTRODUCTION

1.1 The Tiwi Geothermal Field

The Tiwi Geothermal Field has four main sectors – Naglagbong (Nag), Kapipihan (Kap), Matalibong (Mat), and Bariis (Bar), as shown in Figure 1 (Menzies, et al, 2010). Naglagbong, an outflow, was the first sector to be developed. Steam production rapidly declined in the sector in the mid 1980's due to the influx of peripheral fluids, and it is now used as an injection area. Present production is from the three other sectors. South Kapipihan (So Kap) and Bariis are both upflow areas, as well as South Naglagbong. Kapipihan is affected by injection in Naglagbong, although production in South Kapipihan has been stable for the past 35 years. Matalibong, another outflow area, was the main contributor of production in the 1990's, with a number of dry steam and superheated wells. Due to the rise in deep pressures and hence, the steam-liquid interface, most of the sector's current production is low enthalpy two-phase (Calibugan, et al., 2015). This paper focuses on numerical simulation of the South Kapipihan and Matalibong sectors.

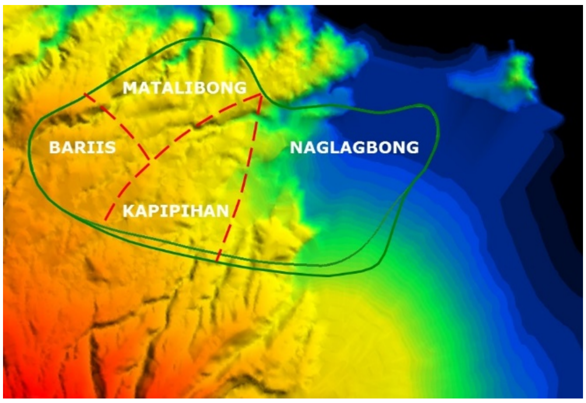

Figure 1: A topographical map of the Tiwi Field. Shown are two versions of the production boundary (green), the larger being the revised one in 2004, and the four sectors: Naglagbong, Kapipihan, Matalibong, and Bariis.

1.2 The Tiwi Numerical Model

The Tiwi Numerical Model is a three-dimensional mathematical representation of the reservoir, based on the TOUGH2 (Transport of Unsaturated Groundwater and Heat) simulation code developed by the Lawrence Berkeley National Laboratory (LBNL). The model uses a double porosity formulation, with various levels of matrix block sub-division (MINC'ing) in the reservoir section. The commercially active reservoir (both production and injection areas) have MINC 5, while the clay cap and the basement rock have single porosity. Double porosity enables the model to simulate both (1) fast reactions of the fracture network to reservoir processes, such as pressure drawdown and injection breakthrough, and (2) slower and protracted changes due to more restricted interaction between the fracture network and the matrices. Capillary pressure is also activated in the matrix blocks to facilitate fracture-matrix mass flows.

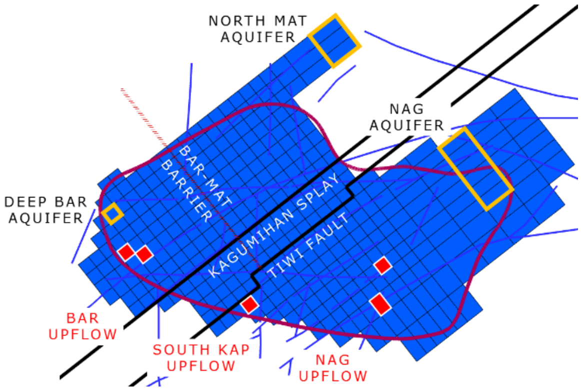

Figure 2: Plan view of Tiwi model showing the upflows (Bar, South Kap, and Nag) as constant rate injection blocks, the constant pressure aquifers (Nag, North Mat, and Deep Bar), and the three structures acting as semi-permeable barriers (Tiwi Fault, Kagumihan Splay, and the Bar-Mat Barrier)

Hot recharge to the model is included as constant rate injection point sources in selected blocks in the bottom layer of the model that correspond to the Bariis, South Kapipihan and South Naglagbong upflows. The inflows remain constant during all phases of modeling. Aquifers (constant pressure blocks) are connected at various locations at the boundary of the model to act as outflows during initial state matching. They may also provide recharge once sufficient pressure drawdown occurs during the production phase. The three aquifers in the model are Northeast Naglagbong, North Matalibong, and Deep Bariis. These features are illustrated in Figure 2. Additional conductive heat is provided at the base of the model and heat loss occurs through the top of the model. The model's active area is from sea level to 3,700 m below sea level (BSL).

The model is orientated northeast-southwest to fit as closely as possible with interpreted geological structures, particularly the Tiwi Fault and Kagumihan Splay, which appear to act as partial barriers to east-west hydrological interactions. Aside from these two faults, another barrier between Bariis and Matalibong (Bar-Mat Barrier) is included in the model, to reflect the different pressure histories of the two sectors.

1.3 Pressure and Enthalpy Matching

The Tiwi Numerical Reservoir Model has been matched to pressure and enthalpy changes using the production and injection data that has been collected during the field's production history. As shown in Figures 3, 4, 5, and 6, historical pressures in Naglagbong, South Kapipihan, and North Matalibong have been sufficiently matched from the late 1970's to the present, before calibration with gravity measurements were started. These are represented by Sim Run 0 in the pressure history plots. (Sim Run 4, the latest model calibrated with gravity, will be discussed in the next section.) All the major dynamic events in the field's production life have been simulated:

(a) the initial pressure drawdown in the eastern part of the field (Naglagbong and Kapipihan in Figures 3 and 4, respectively) due to production in Naglagbong without reinjection in the early 1980's; this includes the expansion and eventual contraction of the shallow steam zone in Naglagbong

(b) the pressure recovery in the east starting from the mid-1980's; see Figures 3 and 4

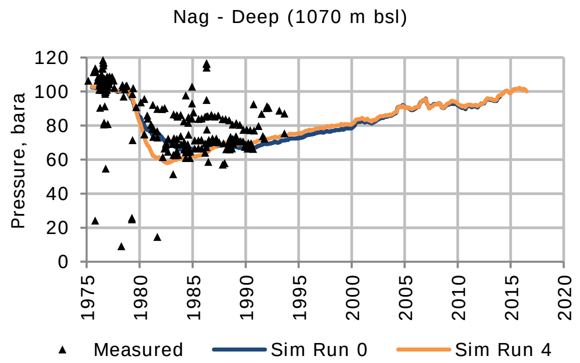

Figure 3: Measured vs. Simulated Pressure history of Naglagbong at Liquid Depth, before gravity matching (Sim Run 0) and latest model calibrated with gravity (Sim Run 4)

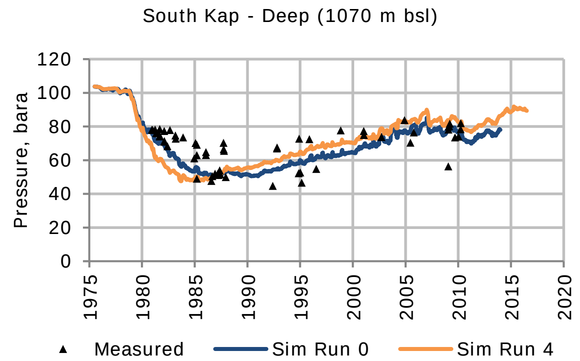

Figure 4: Measured vs. Simulated Pressure history of South Kapipihan at Liquid Depth, before gravity matching (Sim Run 0) and latest model calibrated with gravity (Sim Run 4)

(c) the pressure drawdown in the west (Matalibong, shown in Figures 5 and 6) delayed by 1 to 2 years; this includes the expansion of the steam zone, with its greatest extent in the mid-1990's

(d) the pressure recovery in Matalibong starting from the mid-1990's, also shown in Figures 5 and 6

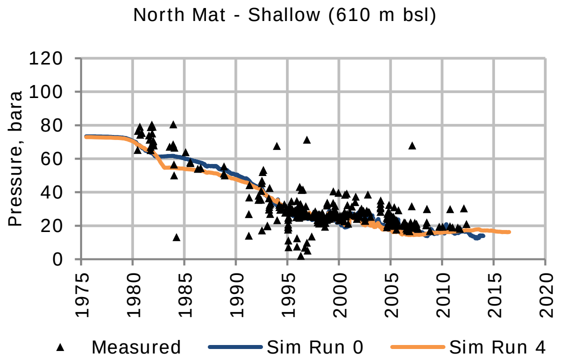

Figure 5: Measured vs. Simulated Pressure history of North Matalibong at Steam Zone Depth, before gravity matching (Sim Run 0) and latest model calibrated with gravity (Sim Run 4)

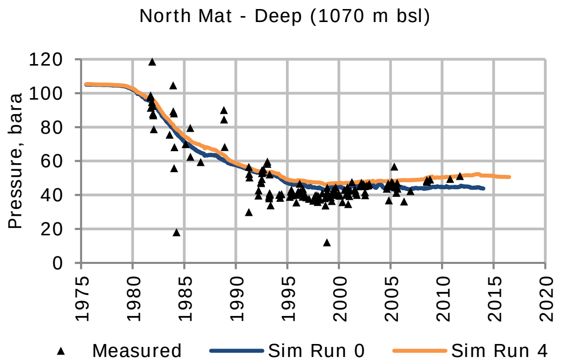

Figure 6: Measured vs. Simulated Pressure history of North Matalibong at Liquid Depth, before gravity matching (Sim Run 0) and latest model calibrated with gravity (Sim Run 4)

Average discharge enthalpies have also been sufficiently matched, particularly in the second half of development history. Shown in Figures 7 and 8 are enthalpies of South Kapipihan and Matalibong, the sectors that shall serve as case studies in this paper. For South Kapipihan, simulation is easier as there is no steam zone in the area.

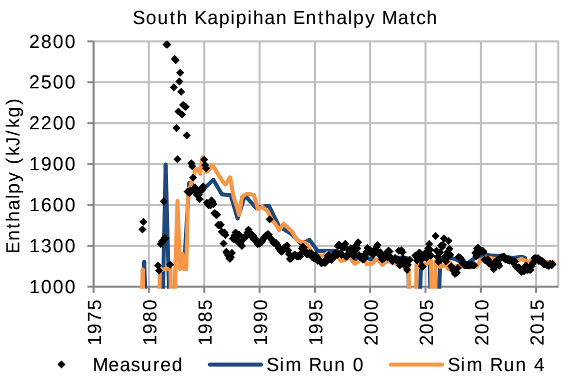

Figure 7: Measured vs. Simulated Average Discharge Enthalpy of South Kapipihan, before gravity matching

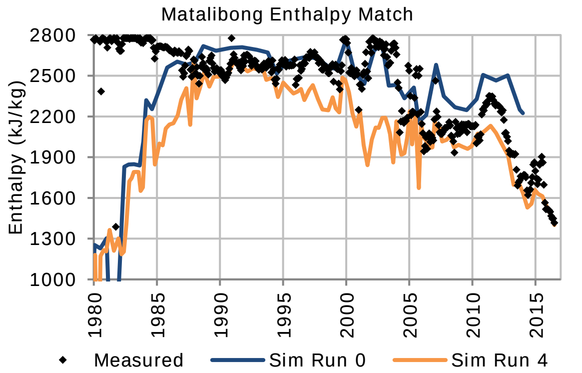

Figure 8: Measured vs. Simulated Average Discharge Enthalpy of Matalibong, before gravity matching

2. GRAVITY MATCHING

Part of the history matching process for numerical models in PGPC is to calibrate to changes in density, as measured in precision gravity surveys. (Atkinson and Pedersen, 1988; San Andres, 1992) The models usually undergo this process after being constrained by good matches in pressures and enthalpies. A model well matched with pressure data from downhole surveys, which are actually the pressures in the fractures, do not necessarily translate to a good match with the mass contained in the reservoir, most of which are residing in the matrices. External sources like constant pressure aquifers in the periphery could of course provide the mass needed to stabilize the liquid pressures after a drawdown due to production, but in order to ascertain the robustness of any numerical model, mass flows (1) between the fracture network and external sources, and (2) between the fractures and matrices, must be both accounted for.

Precision gravity surveys monitor spatial and temporal variations of net mass changes in the reservoir. The variations in mass, measured as density changes, are mainly caused by saturation changes in the porous rock over time due to steam and two-phase production, brine injection, and external aquifer inflow. (Nordquist, et al, 2004; Nordquist, et al, 2010) The entire production and injection area have been covered by surveys since 1982, with the latest, 21st, carried out in 2015. The network is currently composed of 110 benchmarks. Figure 15 illustrates the location of benchmarks that are discussed in this paper.

An initial comparison of the measured and simulated gravity, represented by Run 1 in Figures 9 to 11 (Fig 9 for Benchmark 35 in Mat, Fig 10 for Benchmark 84SAT also in Mat, and Fig 11 for Benchmark 106 in Nag), shows that the mass in the model isn't declining sufficiently during the 1980's, which was the initial production phase in Tiwi, characterized by zero to partial reinjection of produced brine. Likewise, the mass recovery in the latter phase of history is smaller as the reservoir did not lose a lot of mass. This means that the matrices were holding the fluid too much, and the fracture network was getting most of its fluid from external aquifers.

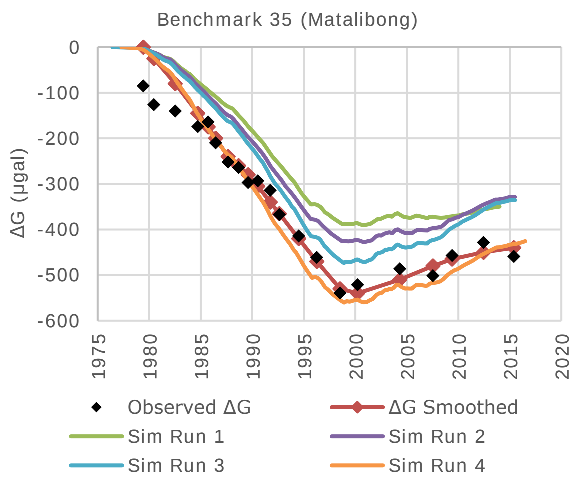

Figure 9: Observed vs. Simulated Change in Gravity in Benchmark 35 (Matalibong).

In Run 2, changes were made in the model to reduce the influence of the North Matalibong and Deep Bariis aquifers relative to the matrix blocks of the model, so that when mass exits the reservoir in the form of production, the amount of replacement fluid sourced from the matrices is increased. This is implemented in the model by reducing the interface area of connection between the aquifer elements, which are outside of the model's grid system, and the blocks they are connected to. This interface area controls the heat and mass flowing between two blocks.

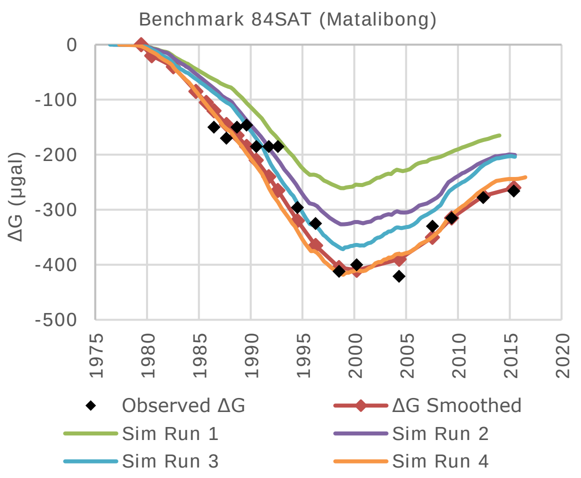

Figure 10: Observed vs. Simulated Change in Gravity in Benchmark 84SAT (Matalibong).

The semi-permeable barrier between Bariis and Matalibong was also adjusted using the same technique with the aquifers, changing the effective interface area of the plane of the barrier. The model, with the aquifer inflows reduced, naturally resulted in lower pressures, so the interface area of the barrier is increased, making the barrier more permeable and allowing the Bariis and Matalibong areas to interact more, without significantly disrupting their respective pressure histories.

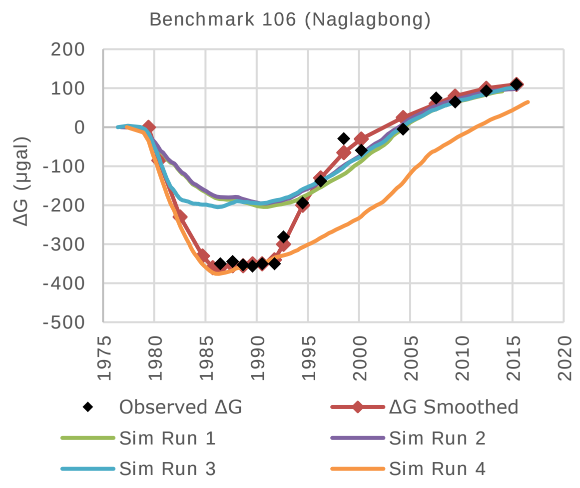

Figure 11: Observed vs. Simulated Change in Gravity in Benchmark 106 (Naglagbong).

For Run 3, the changes involve reducing the fracture spacing of the blocks, the same method used by Nordquist, et al, 2010. The model had 150 m fracture spacing in all areas except for the shallow regions in the west (Bariis and Matalibong); from 600 to 700 m BSL, fracture spacing is 45 m, and from 200 (the shallowest part of the reservoir) to 600 m BSL, it is 30 m. For Run 3, the fracture spacing is further decreased, and the volume of reservoir with small fracture spacing is increased; with 23 m fracture spacing from 200 to 950 m BSL in the west, and from 0 to 600 m BSL in a small area in the extreme northeast, near the Northeast Naglagbong aquifer. This fracture spacing reduction further improved the match to gravity and also improved the match to the average discharge enthalpy in Naglagbong by rapidly flashing more of the shallow region in the early 1980's (Figure 12).

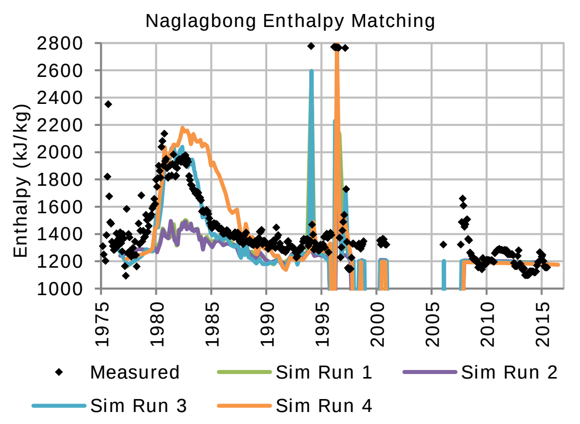

Figure 12: Measured vs. Simulated Average Discharge Enthalpy of Naglagbong

In Run 4, capillary pressure was "turned off" to allow more flow from the matrix to the fractures and this achieved an even faster decline in mass and further improved the match to the gravity data. The manner of increase in Naglagbong, illustrated in Figure 11 may not be the same as observed, but the overall change is fairly matched.

To assist in understanding the various mass sources and sinks that may be affecting the gravity match, a comprehensive diagnostic tool was developed by Parini (2016) to quantify the mass-in-place and fluxes for a given Matalibong volume in the reservoir model. This has been useful during the gravity matching process, to identify which mechanisms need to be adjusted. Figure 13 shows the location of this volume, which extends from the shallowest to the deepest layer of the model. In Figure 14, the mass-in-place in the fractures and the matrices are plotted. The matrices comprise the majority of pore volume, and hence contain most of the fluid mass. Note how the change in mass in the matrices resembles the gravity response of BM 84SAT and to a lesser degree BM 35, in Figures 10 and 9, respectively.

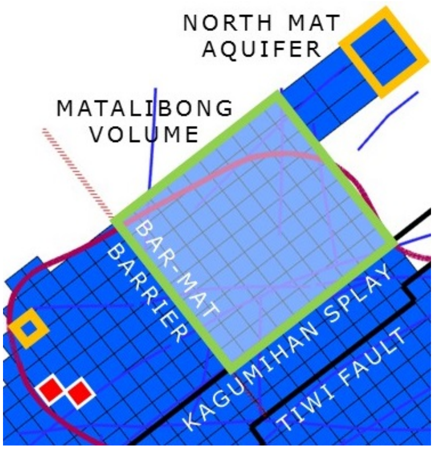

Figure 13: Location of Matalibong volume diagnosed in Figure 14

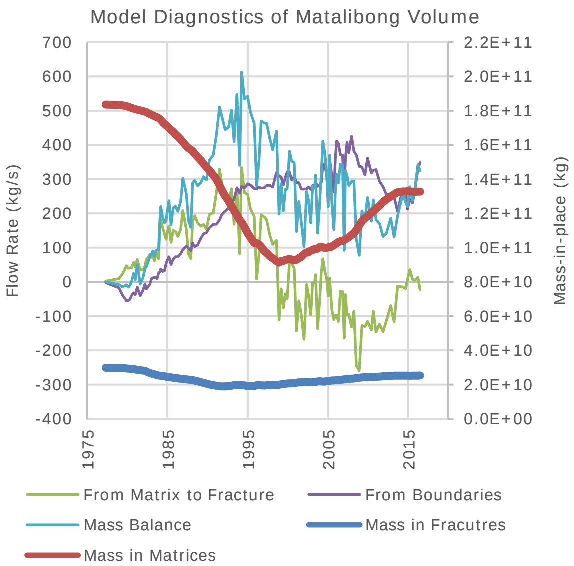

Figure 14: Matalibong volume diagnosed into masses in fractures and matrices, and mass fluxes (extraction through well production, flow between matrix and fractures, and flow through boundaries)

An illuminating plot in Figure 14 is the flow from matrix to fracture (green). The mass from matrices increases up to 1995, then decreases and hovers between zero and negative from 2000 to 2015. This means that for the past 15 years, the fracture network is slowly resaturating the matrices, and that recharge to the fracture network exclusively comes from external sources, in this case from the Mat injection and from the boundaries; the North Mat aquifer, through the Kagumihan Splay, and through the Bar-Mat Barrier from Bariis. The Mass Balance plotted is the difference between the fluid coming from the boundaries and the fluid returning to the matrices. This should be equal to the mass extraction (through well production) and is a good countercheck if inputs are correct.

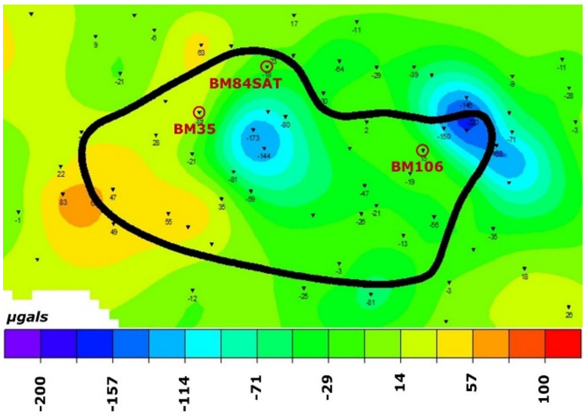

Figure 15: Difference of observed and simulated gravity from 1982 to 2015, labeled with case study benchmarks. (Sim Run 4)

The difference between the observed and simulated gravity for Run 4 is shown in a contour map in Figure 15. Most of the areas are well matched (< ±50 μgals), with the exception of a region in the center of the field, which was never a source of significant production, and the condensate injection area in the northeast. Southwest Bariis is also not well matched, as the model has smaller mass than what is observed. However, Bariis has a deep aquifer that has a constant pressure and temperature, and in terms of asset development, this represents an optimistic case - a prolific source of hot fluid.

3. MICROEARTHQUAKE MONITORING

Another geoscientific data that are used to improve the model are microearthquakes (MEQs). MEQ monitoring in Tiwi has been conducted since the 1980's with the most recent array operational from May 2012 to June 2017. The array consists of 7 to 10 operating stations recording seismic signals using a system of geophones and GPS antennas. The network covered an area of approximately 8 km x 8 km with the stations having a spacing of 2 to 3 km.

In the five years of continuous MEQ monitoring in Tiwi, a total of 6,560 events were recorded within and outside the active geothermal field. Approximately 63% of these events were classified as local, which means that the MEQ's occurred inside the array. The total number of local MEQ's translates to an average of 68 events per month or about 818 events per year. None of the MEQ's measured magnitude three or more, and none were reported as felt. Likewise, no damage to any of PGPC's facilities resulted from MEQ's. These events occur in shallow depths (between 500m and 3,500m) compared with earthquakes of tectonic origin.

As shown in Figure 16, the majority of MEQ's have been located in the South Kapipihan - Central Naglagbong areas. MEQ's in this cluster comprise 56% of all the events that were recorded in Tiwi. The observed spatial and temporal correlation between MEQ's in South Kapipihan and Central Naglagbong and the continuous injection in the Southeast Hot Brine Injection System (SEHBIS) supports the connection between injection and induced seismicity in Tiwi. This interaction has also been observed in the Northern Geysers Reservoir. (Stark, 2003)

MEQ's in South Kapipihan extended deeper with the increased injection in SEHBIS in recent years. The deeply occurring MEQ's indicate stimulation of fractures at depth which suggests that the bottom of the reservoir in South Kapipihan could be deeper than initially thought and is consistent with the model of an upflow in this part of the field. When the conceptual model was updated in 2004, the bottom of the reservoir was defined at around 2,400 m BSL. Data collected from 2012 to 2017 have MEQ's reaching 3,500 m BSL, as shown in Figure 17. This is near the assumed base of the resource used in the numerical model, which is 3,700 m BSL. It is also noted that the period from 2012 to 2014 has deeper MEQ's than 2015 to 2017, suggesting that the deep fracture system may no longer be stressed to critical levels and could have stabilized.

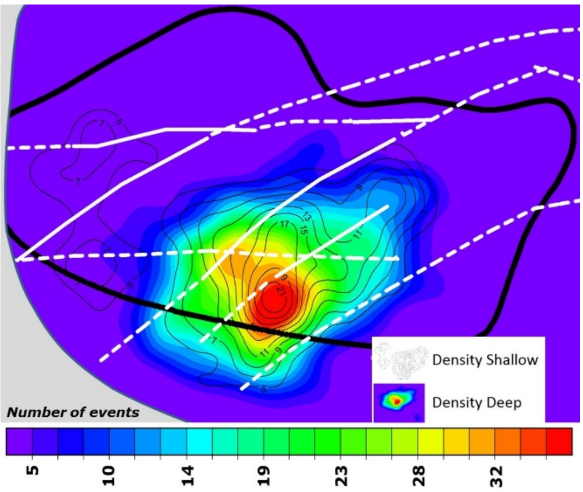

Figure 16: Density of shallow (above 2,000 m bsl) and deep (below 2,000 m bsl) MEQ's, contoured to number of events per 250 x 250 m area

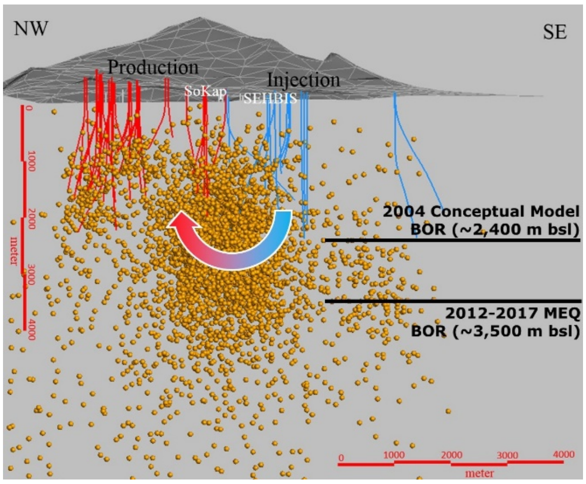

Figure 17: Cross section of Tiwi showing MEQ's recorded from 2012 to 2017

The swarm of MEQ's in South Kapipihan – Central Naglagbong include the hot brine injection area in the southeastern edge of the production boundary, plotted in Figure 17 with blue well tracks. The high MEQ area also includes prolific producers in South Kapipihan, which have less than 3% (annual) decline rates in the past decade. These wells, closest to the South Kapipihan upflow area, are also affected by hot brine injection in Naglagbong, based on geochemical analysis, but have nevertheless maintained their stability over the years.

The presence of MEQs in South Kapipihan confirms the viability of this region as a future drilling area, and also supports the assumption in the numerical model of a permeable volume of reservoir reaching 3,500 m BSL.

4. TRACER INJECTION

Injection in the Naglagbong area, specifically hot brine injection near the southeast edge of the production boundary, has long been known to reach the production wells of the South Kapipihan area. This connection, although observed with various surveillance activities, has not translated into significant decreases in production, owing to the area being an upflow region.

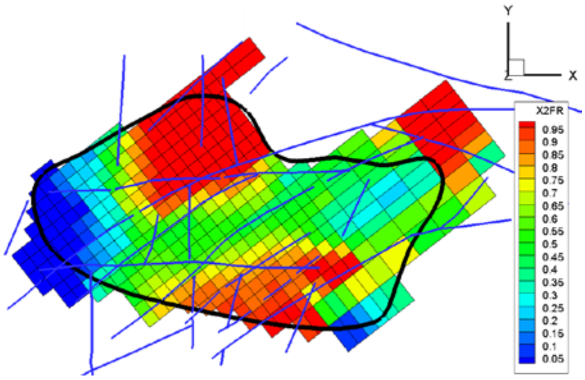

Figure 18: Injectate mass fraction in reservoir model blocks, fracture domain (X2FR) by 2014

In the course of calibrating the model, a question arose whether injectate was reaching production areas, as observed in the field. In order to simulate injectate movement in the reservoir model, it was tagged as "second water" in the two-water option of TOUGH2's Equation of State No. 1. (Pruess, et al., 2011) in a full history run. Figure 18 shows the mass fraction of injectate by 2014, after several years of infield injection. Note that the injectate fraction reaches almost 100% in the three main injection areas (Southeast Naglagbong, Northeast Naglagbong, and North Matalibong), due to the closed boundaries of the model. The results are therefore considered to be representative of how the injection fluid moves through the modeled reservoir but the fractions have not been calibrated against the actual values. However, it added confidence that the model can be used to help in resource management decisions such as the selection and optimization of injection areas.

The model was then used to simulate the effect of lower hot brine injection temperatures in edgefield Naglagbong to South Kapipihan production as a prerequisite of the planned installation of a new binary plant. Initial results suggest that lowering the injectate temperature from 175 deg C to 70, 55, and 40 deg C will have no effect on production.

While the strong upflow region can be an explanation for the lack of response, another dataset for calibration was sought. In 2012, tracer injection tests were conducted on Nag-25 and 31, two of the edgefield injectors. Tracers injected in these two wells were detected in South Kapipihan production wells (Kap-20, 21, 22, 35, and Nag-28). The fastest arrival was 28 days, from Nag-31 to both Kap-21 and Nag-28, with the peak concentration occurring at around 100 days. The two-water run of the model was applied to this test, with the second water (injectate) applied each to Nag-25 and Nag-31 in separate runs. The second water was injected at 10 kg/s for four hours. A high rate was chosen so that clear pulses can be generated. The results show that simulated injectate was too slow in reaching South Kapipihan, with a fastest arrival of 70 days, from Nag-31 to Nag-28, and a peak concentration of more than 200 days. Figures 19 and 20 show measured and simulated tracer returns from Nag-25, respectively. Figures 21 and 22 show measured and simulated tracer returns from Nag-31, respectively.

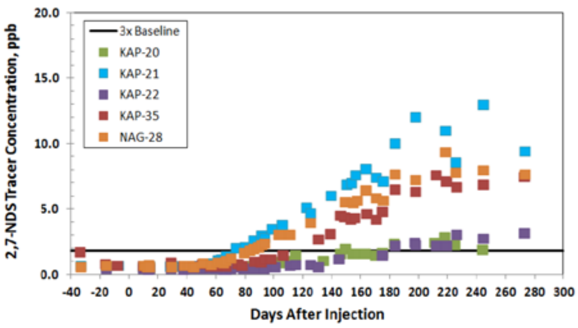

Figure 19: Concentration profiles of Tracer (2,7-Dinaphthalene sulfonate) from Nag-25

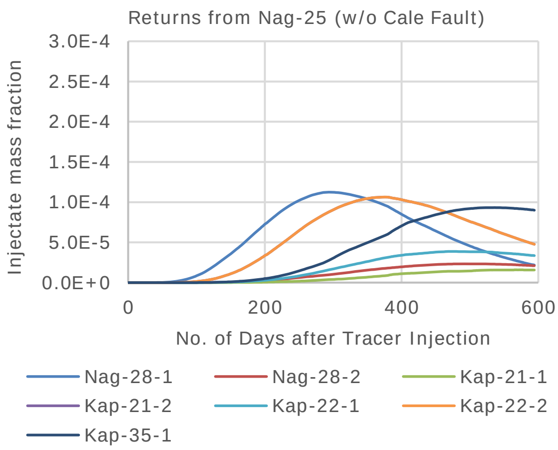

Figure 20: Simulated Nag-25 injectate mass fraction in every feedzone of South Kap wells

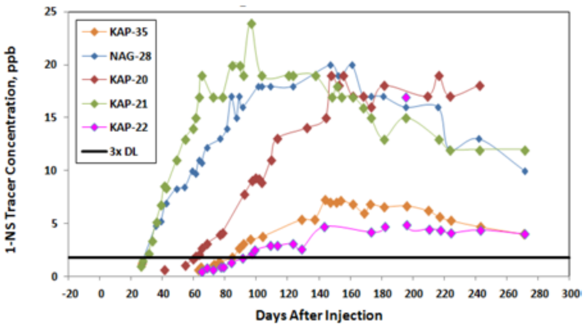

Figure 21: Concentration profiles of Tracer (1-Naphthalene sulfonate) from Nag-31

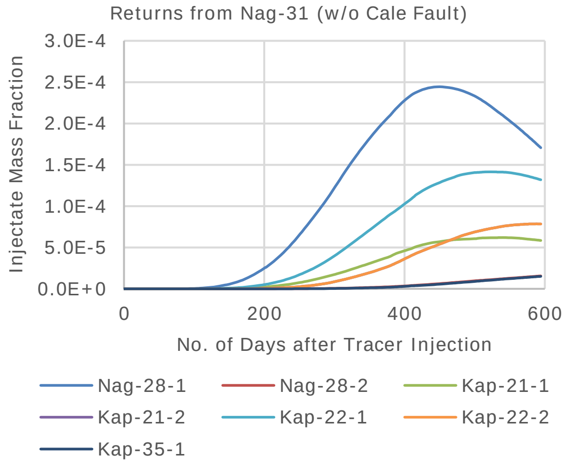

.

Figure 22: Simulated Nag-31 injectate mass fraction in every feedzone of South Kap wells

The results of the simulation run imply that the model is likely to be too optimistic with regard to injection effects on production. The major parameter affecting the arrival times in the model is distance, as there are no structures, such as faults, built into the model in the southeast to enhance permeability and fluid flow therefore only relies on the permeability of the fracture network. Considering the results, it was decided to add the Cale Fault in the model as it is a recognized feature in the southeast part of the field that could be providing an enhanced permeability connection between the injection and production wells. The addition of Cale Fault is not straightforward, however, as the blocks of the reservoir model are orientated with the Tiwi Fault and Kagumihan Splay and the workaround is to represent the fault as a crisscrossing series of blocks. After a number of runs, it was found that a streak of blocks with 1,800-millidarcy horizontal permeability and with a "fence" around it (Figure 23) was required to get a reasonable match to the tracer arrival times. This fence has a heat and mass transfer area multiplier of 0.001 to focus flow within the fault zone. This is required, since tracer from Nag-25 arrived much later in the production wells compared with tracer from Nag-31. Nag-25 is farther from the Cale Fault than Nag-31, which is along its strike. Also, production wells farther from the fault such as Kap-35 have slower arrival times and lower concentrations of tracers. Figures 19 and 21 illustrate the difference in arrival times and concentrations.

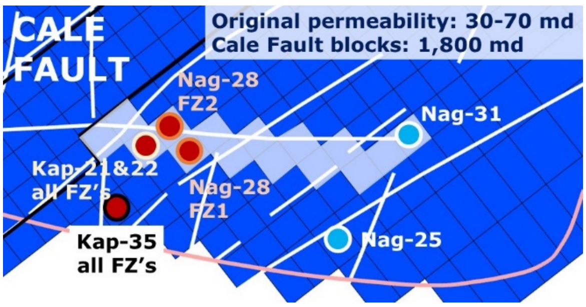

Figure 23: Inclusion of Cale Fault in the reservoir model as a streak of high permeability blocks (inset of southeastern portion of Tiwi model)

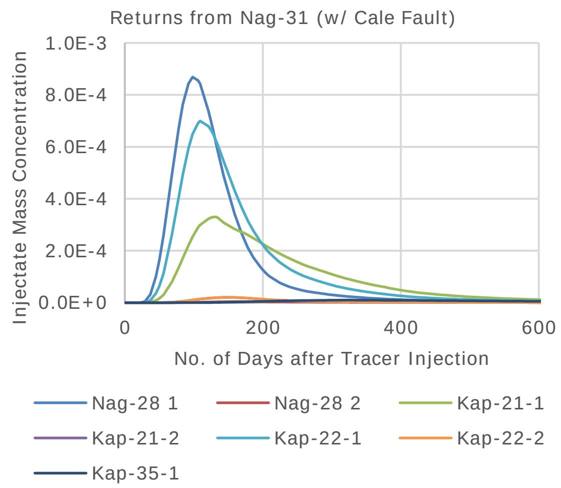

Figure 24: Simulated Nag-31 injectate mass fraction in every feedzone of South Kap wells, from model with Cale Fault

The calculated tracer profiles in the revised model became more consistent with the 2012 tests, as shown in Figure 24. Forecasts were again run, and lower temperature injection was then found to have a more significant effect on production, due to potential cooling from injection wells. However, it was also found that this could be minimized by moving injection further away from the production area.

5. CONCLUSION

The construction of a numerical model is always necessitated by a need to quantitatively assess resource development options and having a well calibrated model improves confidence that the results from analysis of these options can be relied on for making the necessary decisions. In Tiwi's case, significant development options being considered include the gain and effect of drilling new deep wells and the addition of a binary plant to extract more heat from the injected hot brine. The model is also used for other analyses and tasks, such as annual forecasts for business planning needs, gains of workovers, effect of migrating injection to different areas, small projects such as reflowing of idle wells, and other capital projects.

In the course of calibrating the model for these purposes, major features of the conceptual model, such as the upflows, major aquifers, and the most prominent barriers are included, and basic datasets, such as production and injection data, and pressure and temperature measurements, are used. This gives assurance that the mass and energy balance is satisfactorily simulated. However, it is also important that the model be calibrated against as many sets of data as possible, such as precision gravity surveys, microearthquakes, and tracer injection and to accomplish a good match, more features of the conceptual model may be added, such as additional faults and barriers. If properly integrated, these additional features will improve history matching and simulation of various reservoir processes, and increase confidence in the model's output and the use of the model to provide input to resource development decisions.

6. REFERENCES

Atkinson, P. G. and Pedersen, J. R., Using Precision Gravity Data in Geothermal Reservoir Engineering Modeling Studies, Proceedings 13th Stanford Workshop on Geothermal Reservoir Engineering, 35-40 (1988).

Calibugan, A. A., Villaseñor, L. B., Menzies, A. J., and Stark, M. A., An Evaluation of the Impact of MatRidge Injection to Matalibong Production, Tiwi Geothermal Field, Philippines, Proceedings World Geothermal Congress 2015, Melbourne, Australia, (2015).

Menzies, A. J., Villaseñor, L. B., and Sunio, E. G., Tiwi Geothermal Field, Philippines: 30 Years of Commercial Operation, Proceedings World Geothermal Congress 2010, Bali, Indonesia, (2010).

Nordquist, G. A., Protacio, J. A. P., and Acuña, J. A., Precision gravity monitoring of the Bulalo geothermal field, Philippines: independent checks and constraints on numerical simulation, Geothermics 33, 37-56 (2004).

Nordquist, G. A., Acuña, J. A., and Stimac, J. A., Precision Gravity Modeling and Interpretation at the Salak Geothermal Field, Indonesia, Proceedings, World Geothermal Congress 2010, Bali, Indonesia, (2010).

Parini, M. A., personal communication. 2014.

Pruess, K., Oldenburg, C., and Moridis, G.: Tough2 User's Guide, Version 2. LBNL-43134. 2011.

San Andres, R. B., Precision Gravity Monitoring at the Tiwi Geothermal Field, Philippines, Proceedings 14th New Zealand Geothermal Workshop, Auckland, New Zealand, (1992).

Stark, M. A., Seismic Evidence for a long-lived Enhanced Geothermal System (EGS) in the Northern Geysers Reservoir, Geothermal Resources Council Transactions, Vol. 27 (2003).